MODELLING THE CARDIOVASCULAR SYSTEM FOR AUTOMATIC INTERPRETATION OF THE BLOOD PRESSURE CURVE

TIM MYERS, ANNA SÁEZ DE TEJADA, VICENT RIBAS RIPOLL, SARAH MITCHELL, AND MARK J. MCGUINNESS

Abstract

A four compartment model of the cardiovascular system is developed. To allow for easy interpretation and to minimise the number of parameters, an effort was made to keep the model as simple as possible. A sensitivity analysis is first carried out to determine which are the most important model parameters to characterise the blood pressure signal. A four stage process is then described which accurately determines all parameter values. This process is applied to data from three patients and good agreement is shown in all cases.

1. Introduction

The human cardiovascular system conveys nutrients and oxygen to tissues and maintains the gas and fluid exchange with tissue that is necessary for homeostasis. The health of this system is important, and diagnosing cardiovascular problems in a timely and non-invasive manner is a matter of significant medical interest. A key indicator of cardiovascular health is the blood pressure and the way that it varies with time.

The term blood pressure refers to the force per unit area that blood exerts on the walls of blood vessels. This force changes both in time and with the effective distance from the aortic arch. Systolic pressure is the highest pressure, observed during ventricular contraction, whilst diastolic pressure is the lowest/baseline pressure reached during ventricular relaxation (diastole) [12]. Currently there exist two principal methods for measuring blood pressure:

- The sphygmomanometer – this is the standard cuff which is usually inflated on the upper arm, and allows the assessment of systolic and diastolic blood pressures through the presence/absence of Korotkoff sounds (pulse) or of oscillations above mean pressure (oscillometric) . In general it is manually operated and requires a quiet environment. It is an old technology (from the 1800s) that is prone to operator error. It also provides data only for a short period. Whilst digital cuffs exist these may be highly inaccurate.

CRM Preprint Series number 1129

- The catheter – this is inserted into an artery and provides continuous blood pressure data that reveals more than the cuff about the state of the cardiovascular system. However, it is an invasive technique which has a number of associated risks and so is primarily used on critical or surgical patients.

There is much interest in developing a reliable non-invasive, continuous monitoring technique for blood pressure, and various research groups have tackled this problem by different methods. One such approach involves the use of the pulse oximeter [19]. This has particular appeal since the pulse oximeter is already standard equipment in most medical practices.

The pulse oximeter is a device currently used to measure the oxygen saturation of the blood. Typically it functions by shining two lights, of different wavelength (but both close to infra-red) through a translucent part of the body. The different wavelength lights are absorbed, to differing degrees, by the oxygenated and deoxygenated haemoglobin and so the ratio of oxygenation to deoxygenation may be calculated. Since arterial (oxygenated) blood vessels respond to pressure changes more than the venous (de-oxygenated) system, the obtained signal is time-dependent and so the output of the pulse oximeter is closely related to the peripheral arterial blood pressure, and may also be used to monitor the heart rate. In fact this variation in the signal is essential to the functioning of the device since, to distinguish the light absorption from the blood and surrounding tissue, the pulse oximeter uses the varying part of the signal.

The output from the pulse oximeter is termed the photoplethysmograph (pleth). The pleth closely resembles the blood pressure curve. Currently the main uses of the pulse oximeter are oxygenation and heart rate monitoring. However, the detailed features of the blood pressure curve and hence the pleth contain a wealth of information useful for diagnostic purposes. For example the blood pressure curve may be used for:

(1) Detection of cardiac arrhythmias;
(2) Measuring cardiac output;
(3) Measuring hypovolemia;
(4) Monitoring respiratory variation (which in turn may be related to fluid responsiveness in ventilated patients with circulatory failure);
(5) Detecting attenuation of the peripheral pulse waveform — depending on different base pathologies such as sepsis or severe respiratory distress, such attenuation/damping may be considered an important measure for the assessment of microcirculation and tissue perfusion.

More comprehensive lists of examples of clinical uses for a detailed blood pressure curve may be found in [5, 18, 21, 22].

Until recently it has not been possible to accurately relate the pleth to the blood pressure, since the scaling depends on compliance, or parameters related to it such as age, weight (obesity), and gender, as well as other factors. This

CRM Preprint Series number 1129

problem has been addressed by researchers at Sabirmedical using a random forest algorithm [19]. Unfortunately, although physicians are able to interpret it, the random forest approach does not provide an understanding of the physiological mechanisms behind the pleth. At two meetings, held in the Centre de Recerca Matemática in 2010, mathematicians were challenged to develop an accurate physiological model of the cardiovascular system in order to better understand the pleth and so extract further information. This would allow the pulse oximeter to be used as an automatic diagnostic tool, so reducing operator error and allowing less highly trained operators to perform preliminary diagnoses. The following work results from those meetings.

The specific goal of this paper is then to produce a mathematical model capable of accurately reproducing the dominant features of the blood pressure curve and in particular the dicrotic notch associated with aortic valve closure, and the variation due to respiratory sinus arrhythmia (RSA). To allow for easy interpretation and to minimise the number of parameters, an effort was made to keep the model as simple as possible. In the following section we will describe the compartment approach that was used to model the human cardiovascular system. Subsequent sections deal with model refinements and parameter estimation. Finally we compare our model results with data.

2. Basic compartment models

The main components of the cardiovascular system are the heart, arteries and veins. It includes the pulmonary circulation, a closed loop through the lungs where blood is oxygenated, and the systemic circulation. Oxygenated blood enters the systemic system at the left heart and is then pumped into the aorta. The aorta branches into smaller arteries, arterioles and capillaries, where oxygen exchange takes place, and enters the systemic veins through which it flows in vessels of progressively increasing size toward the right heart. The right heart pumps CO_2 rich blood into the lungs, closing the loop.

Differential equation models of the cardiovascular system vary from a pair of first order ordinary differential equations [15] to systems of more than 40 coupled differential-delay equations [24, 25, 9, 8]. Ottesen's approach [15] is to split the system into arterial and venous compartments, with non-pulsatile flow, and a source term that models the effect of the left ventricle. At the other end of the spectrum, Ursino *et al* and Grodins [9, 24, 25] describe the pulsatile flow of blood through multiple compartments including the lungs, compliant arteries and veins and driven by a heart that is regulated by a sophisticated nervous feedback control system that responds to blood pressure and chemistry in a variety of ways. Despite this level of complexity, in general compartment models are conceptually quite simple. They involve dividing the cardiovascular system into a number of compliant zones or compartments and as the blood passes through each zone, blood should be conserved. The change in volume in each zone is simply the

difference between the flux entering from upstream and that leaving downstream. The heart drives this flux and the flow is resisted by the vessels through the shear stress at vessel walls.

In the present study we have tried to take the simplest approach possible, along the lines of Ottesen's model. Initially we employed a three compartment model, involving the arteries, veins and left ventricle. However, one of our main goals was to have our model exhibit a dicrotic notch in arterial pressure. The dicrotic notch is the name given to the pressure pulse seen when the aortic valve closes. This closure is caused by the pressure drop across the valve becoming negative. The size and location in time of the notch provides important information about the health of the valve. In the three-compartment model the arterial pressure is an average across the whole arterial system, so that using this as a measure of when the valve closes leads to late closure in the model, and a temporarily reversed blood flow throughout the arterial system.To improve this behaviour, we introduced a new compartment to describe the exit region close to the valve. Mathematically speaking, there is no problem in dividing the cardiovascular system into any number of compartments, as is done with finite element computations. Nevertheless, to give a physical meaning to this new compartment one could think of it as representing the aortic arch. Our basic model is therefore described by the following four-compartment system

$$(1) \qquad \dot{V}_e = Q_{LV} - Q_e \quad \dot{V}_a = Q_e - Q_a \quad \dot{V}_v = Q_a - Q_v \quad \dot{V}_{LV} = Q_v - Q_{LV} \ ,$$

where V_i represents the volume, and Q_i the flux, of blood. The subscripts e, a, v, LV represent exit, arterial, venous and left ventricle and dots indicate the derivative with respect to time. The first equation indicates that the rate of change of volume in the exit region depends on the difference between the rates at which fluid flows in from the left ventricle and fluid flows out of the aortic arch. In the arteries the volume increases due to fluid flowing in from the arch and decreases as it flows out of the arteries into the veins, leading to the second equation. The third equation expresses a similar material balance for the venous system, and the fourth equation for the left ventricle.

Hence these equations express conservation of blood volume. Summing the four we find $\dot{V}_e + \dot{V}_a + \dot{V}_v + \dot{V}_{LV} = 0$, so the total volume is constant. Note, we assume the blood to be incompressible, see [17] — changes in pressure are associated with the compliance of blood vessels rather than the relatively small compressibility of blood itself, and conservation of blood volume is equivalent to the more fundamental principle of conservation of blood mass.

In a compliant elastic vessel we may relate the pressure difference from ambient, p, to the volume via $V = V_0 + Cp$, where C is a constant, termed the compliance, and V_0 is a constant giving the volume at ambient pressure $p = 0$ (the value of the compliance is discussed in detail later). This equation serves to define the compliance.

CRM Preprint Series number 1129

Special attention is paid to the left ventricle, where the pumping of the heart is driven by changes in the elastance (the inverse of the compliance). Consequently, in the left ventricle we write $V = V_0 + p/E_{LV}$. This equation provides a definition of elastance E as the change in pressure divided by the change in volume — it is analogous to the spring constant in Hooke's law which is defined by the change in force divided by the change in length. Differentiating the compliance and elastance definitions, we can relate volume and pressure as

$$\dot{V}_e = C_e \dot{p}_e \qquad \dot{V}_a = C_a \dot{p}_a \qquad \dot{V}_v = C_v \dot{p}_v \qquad \dot{V}_{LV} = \frac{d}{dt}\left(\frac{p_{LV}}{E_{LV}}\right). \tag{2}$$

Note, we assume that the compliance of the blood vessels is a constant whereas the elastance, representing the contraction of the heart muscle, is a controlled variable that varies in a prescribed manner with time [23]. We may relate the fluxes to the pressure by considering standard, uni-directional pressure-driven laminar flow (Poiseuille flow) in a pipe which leads to a relation of the form $Q \propto \Delta p$. This may be expressed as $Q = \Delta p/R$ where R can be thought of as the effective resistance to flow [12]. Obviously the cardiovascular system does not consist of a single straight pipe and blood flow is often turbulent so this definition of Q is rather approximate and the resistance R must represent the many intricacies of the system, rather than simply the viscous resistance from the classical Poiseuille flow model. With the fluxes written in terms of the pressure drop our initial system of differential equations may now be expressed as

$$C_e \dot{p}_e = \frac{p_{LV} - p_e}{R_e} - \frac{p_e - p_a}{R_a} \tag{3}$$

$$C_a \dot{p}_a = \frac{p_e - p_a}{R_a} - \frac{p_a - p_v}{R_c} \tag{4}$$

$$C_v \dot{p}_v = \frac{p_a - p_v}{R_c} - \frac{p_v - p_{LV}}{R_v} \tag{5}$$

$$\frac{d}{dt}\left(\frac{p_{LV}}{E_{LV}}\right) = \frac{p_v - p_{LV}}{R_v} - \frac{p_{LV} - p_e}{R_e}\,. \tag{6}$$

3. Model refinements

The above system, equations (3 – 6), constitutes our basic set of equations but still requires certain refinement: the driving mechanism for the flow is not defined, neither is there a mechanism to describe the dicrotic notch or the aortic valve.

The driving mechanism for the flow comes through the definition of the elastance, which serves as a simple model of the pumping action of the heart muscle. Modelling of the elastance is discussed in a number of papers. Whilst there is some difference in the fine detail, the general form is of a sequence of roughly Gaussian curves when contraction occurs, separated by flat regions denoting the relaxation [6, 14, 16]. In [8] the elastance has an approximately square wave form.

CRM Preprint Series number 1129

However Suga [23] points out that a more gradual rise in elastance is essential if it is to be consistent with the Fenn effect in cardiac muscle, where the shortening of muscle produces heat.

The elastance also commonly exhibits a longer term variation which is one of the main causes of Respiratory Sinus Arrhythmia (RSA) [3]. RSA is a term for observed changes in heart rate associated with respiration. Heart rate is usually observed to increase during inspiration, and decrease during expiration. This is primarily due to a coupling through the vagal nervous system, and to a lesser extent is also due to the effect of breathing on the pressure in the chest cavity near the heart and to changes in peripheral tone. Denervated (transplanted) human hearts do still exhibit RSA but at around 7.9% of normal levels [2]. Dat [6] models the elastance as

$$E_{LV} = E_d + a(t)(E_s - E_d) \tag{7}$$

where the diastolic elastance E_d is constant and $a(t) = \sin^2(\omega t)$.

We employ the same form as Dat but with two important refinements. Firstly, $a(t)$ should switch off for about 2/3 of the heart cycle (e.g. [24]). If T represents the period of one heart-beat, then we want the $a(t)$ term to rise from zero and fall back to zero once as t varies from a starting value t_0 to $t_0 + \phi T$, where $\phi \approx 1/3$. So we set $\omega = 2\pi/T$ and define $T_{sys} = \phi T$, $T_{dia} = (1-\phi)T$,

$$a(t) = \begin{cases} \sin^2(3\omega(t-t_0)/2)\,, & t - t_0 \in (0, T_{sys}) \\ 0\,, & t - t_0 \in (T_{sys}, T) \end{cases}$$

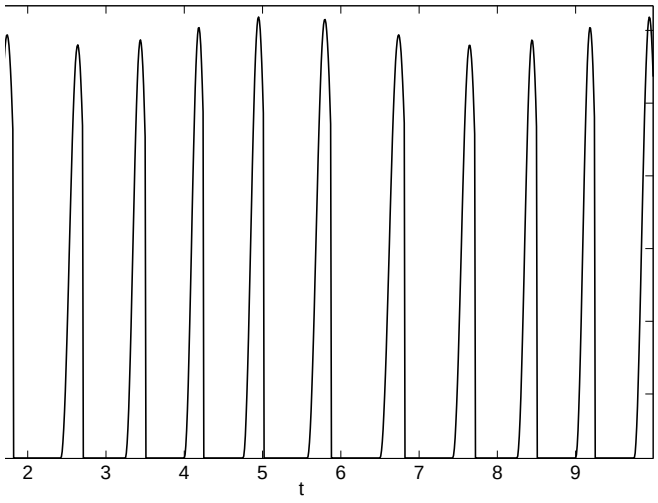

FIGURE 1. Variation of elastance with time

The period T is set to be time dependent, to model RSA with heart rate varying with respiration, by choosing

$$\omega = \omega_0 + c_3 \sin\left(\frac{\omega_0 t}{c_2}\right) . \tag{8}$$

Secondly, the peak in the elastance height also varies over the longer time-scale associated with RSA. To account for this we take the systolic elastance

$$E_s = E_{s0} + c_1 \sin\left(\frac{\omega_0 t}{c_2}\right) . \tag{9}$$

The constants in the above definitions c_1, c_2, c_3 represent half the variation of elastance height, the number of heart beats per respiration (typically around 5) and half the variation of ω respectively. The constant ω_0 is an angular frequency $\omega_0 = (2\pi/60) \times HR$ where HR is an average heart rate in beats/minute.

A typical form for the elastance is shown in Figure 1. The minimum value $E_d = 0.06$mm Hg/ml, while the maximum value varies according to equation (9) with an average value $E_{s0} = 3$mm Hg/ml. We took a heart rate of 72 beats/minute to give $\omega_0 \approx 7.54$. Other parameter values used to generate this graph are given in Table 1.

Parameter	Value	Units	Parameter	Value	Units
C_e	1.5	ml/mmHg	C_a	1.5	ml/mmHg
C_v	50	ml/mmHg	R_{e0}	0.016	s·mmHg/ml
R_a	0.06	s·mmHg/ml	R_c	1.2	s·mmHg/ml
R_v	0.016	s·mmHg/ml	T_{sys}	$T/3$	s
T_{dia}	$2T/3$	s	T	0.9	s
E_d	0.06	mmHg/ml	E_{s0}	3.0	mmHg/ml
ϵ	10^{-5}		A	0.5	
R_{eM}	10	s·mmHg/ml	c_1	0.1	mmHg/ml
c_2	6	beats/breath	c_3	0.01	s^{-1}
c_4	500		c_5	$4 \log 100$	
c_6	7.5		ω_0	7.54	

TABLE 1. Typical parameter values.

The resistances R_a, R_c, R_v are constant while R_e accounts for the aortic valve, that closes when the pressure drop becomes negative. Consequently R_e must be time-dependent. Since closure depends on the pressure difference we write

$$R_e = R_{e0}\left[1 + \epsilon_1(\exp(-A_1(p_{LV} - p_e))\right] \tag{10}$$

CRM Preprint Series number 1129

where R_{e0} is the constant value when the valve is fully open. The factor $\epsilon_1 \ll 1$ ensures that the exponential term remains small whenever $p_{LV} - p_e > 0$ but it increases rapidly when $p_{LV} - p_e < 0$. The constant A_1 is chosen such that the product $A_1(p_{LV} - p_e)$ rises sufficiently rapidly as the valve closes. In practice we set $\epsilon = 10^{-5}$, $A = \frac{1}{2}$: these values are simply chosen to provide the correct properties. Since the exit region is significantly shorter than the arterial region we also assume $R_{e0} \ll R_a$. Another option would be to simply set a switch via a Heaviside function. However, our subsequent numerical calculations showed that this led to a poor representation of the pressure around the dicrotic notch. Ellwein *et al* [7] employ a similar, but cut-off, exponential representation for all heart valves. They do not include the factor $\epsilon_1 \ll 1$ but choose $A = 2$ which is greater than our value, and this has a similar effect. The typical behaviour of the valve is shown in Figure 2.

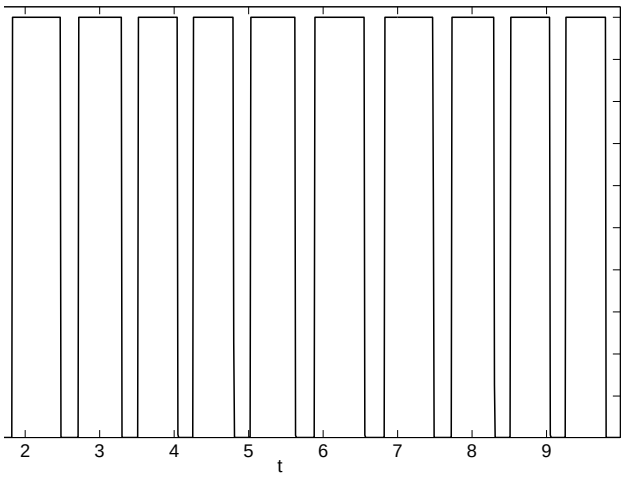

FIGURE 2. Valve resistance against time

Note, we could equally well define a valve at the entrance to the ventricle through

$$R_v = R_{v0}\left[1 + \epsilon_2(\exp(-A_2(p_v - p_{LV}))\right] . \tag{11}$$

However, since this region is of lesser interest to avoid more parameter estimation we use a Heaviside function for R_v (tests confirm this makes no noticeable difference to the results).

The modelling of the dicrotic notch is based on the assumption that it is caused when blood attempting to flow back through the valve, due to a negative pressure difference and inertia, closes the valve and causes stretching and recoil in the valve and supporting tissues, so that blood rebounds into the exit region. Details of momentum build-up and recoil may be found, e.g., in [11]. We approximate this impulse as a Gaussian, with a strength related to the pressure difference $p_e - p_{LV}$.

Since pressure is a function of time we can represent the impulse by the following function

$$f(t) = c_4 \exp(-c_5(t - t_n - c_6\Delta t)^2/(\Delta t)^2)\,. \tag{12}$$

The constants c_4, c_5, c_6 indicate the height of the pulse, the sharpness and the position of the centre. The times t_n, $n = 1, 2, \ldots$, are when $p_e = p_{LV}$ and so indicate when the valve should begin closing. The maximum value of f occurs when $t = t_n + \Delta t$ hence Δt denotes the delay in closure after the pressure drop becomes negative. It therefore controls the position of the dicrotic notch and is an important indicator of the health of the valve. In the numerical solution we use a value of Δt from the previous cycle, and the first value is taken as some typical value.

The function $f(t)$ represents an input of mass to the p_e equation and so is added to equation (3): to conserve mass it must be subtracted from the left ventricle, equation (6). In general its maximum value is much lower than the other terms in the equation and so it represents only a small contribution to the pressure. The full system to model the pressure is now given by equations (4,5) and

$$C_e\dot{p}_e = \frac{p_{LV} - p_e}{R_e(t)} - \frac{p_e - p_a}{R_a} + f(t) \tag{13}$$

$$\frac{d}{dt}\left(\frac{p_{LV}}{E_{LV}(t)}\right) = \frac{p_v - p_{LV}}{R_v} - \frac{p_{LV} - p_e}{R_e(t)} - f(t)\ , \tag{14}$$

with E_{LV} defined by (7) and R_e by (10).

4. Calculating parameter values

Key to the success of the mathematical model is the choice of parameter values. Obviously this is not a simple task given that there are twenty-one parameter values as well as four initial conditions. A number of these values may be estimated from a given pressure signal. For example rearranging the volume pressure relation discussed in §2 we find

$$C = \frac{V - V_0}{p}\,. \tag{15}$$

This may be interpreted as the stroke volume (SV) to mean average pressure, see [12]. According to [1], it may be interpreted as the ratio of stroke volume to arterial pulse pressure. Since we have data for the arterial pressure we may calculate

$$C_a = \frac{SV}{P_{a,sys} - P_{a,dia}}\,. \tag{16}$$

We then use this to estimate $C_e = C_a$ and $C_v = 20C_a$. Note that the value of 20 assumed here for the ratio of venous to arterial compliance is consistent with a number of other studies, including [10] who cite a ratio of 8, [12] who cite a ratio of 24, [24] who uses 33, and a range of 10–20 in [13].

CRM Preprint Series number 1129

Similarly, the systemic resistance may be estimated from the arterial pressure signal, see [1]. Typical values for other parameter values are given the literature, see [6, 8, 15] for example. However, we require parameter values appropriate for specific patients and the values quoted in the literature may be far from those appropriate for a given patient. Experience informs us that if we attempt to fit a blood pressure data set directly by varying all of the model parameter values at the same time (using for example the built-in Matlab function *fminsearch*) then the solution will not converge. Consequently we first carried out a sensitivity analysis to determine which parameters were the most important (in the sense of having the greatest effect on the model's output) and then used these in a four-stage algorithm to determine model parameter values that fit data more accurately.

4.1. **Sensitivity analysis.** Our data sets involve direct measurements of the arterial pressure so this is the pressure we use in the following analysis. The sensitivity analysis consisted in perturbing each parameter of the model and integrating the system of equations to see how the resulting arterial pressure changes with such perturbations. This approach is based on the procedure described in [4].

For each parameter θ, with nominal value θ_0, and for a given perturbation q, the system was integrated for $\theta = (1-q)\theta_0$ and $\theta = (1+q)\theta_0$, while all the other parameters were set to their respective nominal values. Let $p_a\big((1-q)\theta_0\big)$ and $p_a\big((1+q)\theta_0\big)$ be the output arterial pressures for a perturbed parameter θ. Five values of the perturbation q were used: 0.01, 0.05, 0.1, 0.2 and 0.5. The perturbation $q = 0.01$ led to very small changes in the output signal, the perturbation $q = 0.5$ led to chaotic behaviour for some of the parameters. In consequence, these two values were dismissed and only the other three were used for the analysis. In Figure 3 we present two pressure signals, $p_a\big((1-q)\theta_0\big)$ and $p_a\big((1+q)\theta_0\big)$, where the perturbed parameter was $\theta = R_c$ and the perturbation value was $q = 0.1$. From this we can see that varying the value of R_c by a small amount makes significant differences to the pressure signal.

In the following we will measure the influence of the parameters through the L_2 distance between both signals,

$$\delta_2 = \left(\int_0^{20T} \Big(p_a\big((1+q)\theta_0\big) - p_a\big((1-q)\theta_0\big) \Big)^2 \right)^{\frac{1}{2}}. \tag{17}$$

The measure was taken over a signal window of 20 beats, sufficiently far from the initial condition that the signal had settled down. In Table 2 we present the L_2 distances for each parameter and the three perturbations. To reduce the calculations we note that there are a number of parameters that are related, $C_v = 1/E_d$, $C_a = C_e = 1/E_{s0}$, $R_v = R_{e0}$ and $p_e(0) = p_{LV}(0) = p_a(0) = p_{a0}$. Of these only the parameter with the largest L_2 distance is shown in the table. In the thesis [20] two other measures are used: the integrated absolute difference of

CRM Preprint Series number 1129

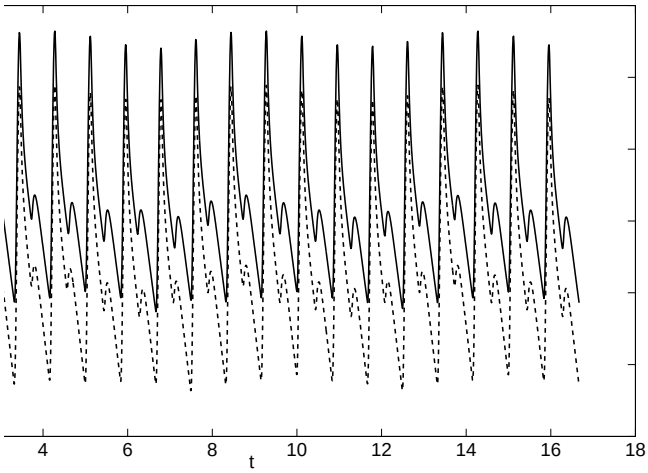

FIGURE 3. Signals for a perturbation 0.1 of R_c

each signal's mean value and the integrated absolute difference of each signal's standard deviation. These give a very similar ordering to that found by the L_2 distance.

From Table 2 and the results described in [20] we deduce the 6 most important parameters to be: 1. E_d (and C_v); 2. E_{s0} (and C_a, C_e); 3. $p_a(0)$ (and $p_e(0), p_{LV}(0)$); 4. A; 5. R_c; 6. ω_0. The final parameter ω_0 is not estimated, since it may be calculated directly from the pressure signal. Consequently in the following section we begin by estimating the remaining top five parameters and subsequently make adjustments to the remaining parameter values.

4.2. **Parameter estimation.** The four stage method used to determine parameters values is described in detail in [20] so we only provide a brief outline below.

In Table 1 we present the set of parameter values used at the beginning of each calculation. The majority of these values are taken from [6, 8, 15] although some, such as ϵ are simply educated guesses. A number of parameter values are read from the data, such as $p_{a0}, p_{v0}, \phi, \Delta t_0$ and so these are not included in the table.

4.2.1. *Stage 1: Approximate Gradient Descent method for the five significant parameters.* We begin by using a Gradient Descent method to find better estimates for the five most important parameters. If $p_a = p_a(t)$ is the arterial pressure signal obtained by integration of the model with a certain set of parameters and $\hat{p}_a = \hat{p}_a(t)$ the arterial pressure signal recorded from a patient then we look to minimize two objective functions involving the mean and standard deviation of the signal:

$$\delta_\mu = \left|\mu(p_a) - \mu(\hat{p_a})\right| \qquad \delta_\sigma = \left|\sigma(p_a) - \sigma(\hat{p_a})\right|. \tag{18}$$

$q = 0.05$		$q = 0.1$		$q = 0.2$	
E_d	22.66	E_d	32.26	E_d	39.52
p_{a0}	20.27	p_{a0}	28.73	p_{a0}	34.90
ϕ	19.75	ϕ	20.35	E_{s0}	28.41
ω_0	10.10	E_{s0}	20.01	A	20.23
E_{s0}	14.17	ω_0	17.75	ω_0	20.10
R_c	9.92	R_c	14.04	R_c	20.04
A	9.69	A	13.81	ϕ	19.66
R_{e0}	7.09	R_{e0}	9.93	R_{e0}	14.11
c_2	6.19	p_{v0}	7.23	p_{v0}	10.20
p_{v0}	5.15	c_6	6.51	R_a	9.16
c_6	4.78	R_a	6.49	c_6	8.60
R_a	4.62	c_4	5.88	c_4	8.35
c_4	4.16	c_2	5.37	c_2	6.81
c_3	3.18	c_5	4.16	c_5	5.94
ε	3.17	ε	4.13	ε	5.76
c_5	2.94	c_3	3.64	R_{eM}	4.70
R_{eM}	2.23	R_{eM}	3.51	c_3	4.32
c_1	1.28	c_1	1.81	c_1	2.56
Δt_0	0	Δt_0	0	Δt_0	0

TABLE 2. L_2 distance between arterial pressure signals for each parameter and perturbation. The parameters have been listed in decreasing order of importance, for each degree of perturbation q.

CRM Preprint Series number 1129

The Gradient Descent method with an objective function $F(x)$ and an initial vector $\mathbf{x}_0$ involves iterating as follows:

$$\mathbf{x}_{n+1} = \mathbf{x}_n - \alpha \nabla F(\mathbf{x}_n)\,, \tag{19}$$

where we take the step-size $\alpha = 0.001$. For the current problem there is no explicit expression for the objective function and so we use an approximate method to determine the gradient with respect to each unknown parameter. Taking C_v as an example, we define $C_{v1} = 1.1 \cdot 50$, $C_{v2} = 0.9 \cdot 50$, and note that $C_v = 50$ is the value quoted in Table 1. The derivative of μ with respect to C_v is approximated by

$$\frac{\partial \mu}{\partial C_v} \approx \frac{\mu\left(p_a|_{C_v=C_{v1}}\right) - \mu\left(p_a|_{C_v=C_{v2}}\right)}{C_{v1} - C_{v2}}\,. \tag{20}$$

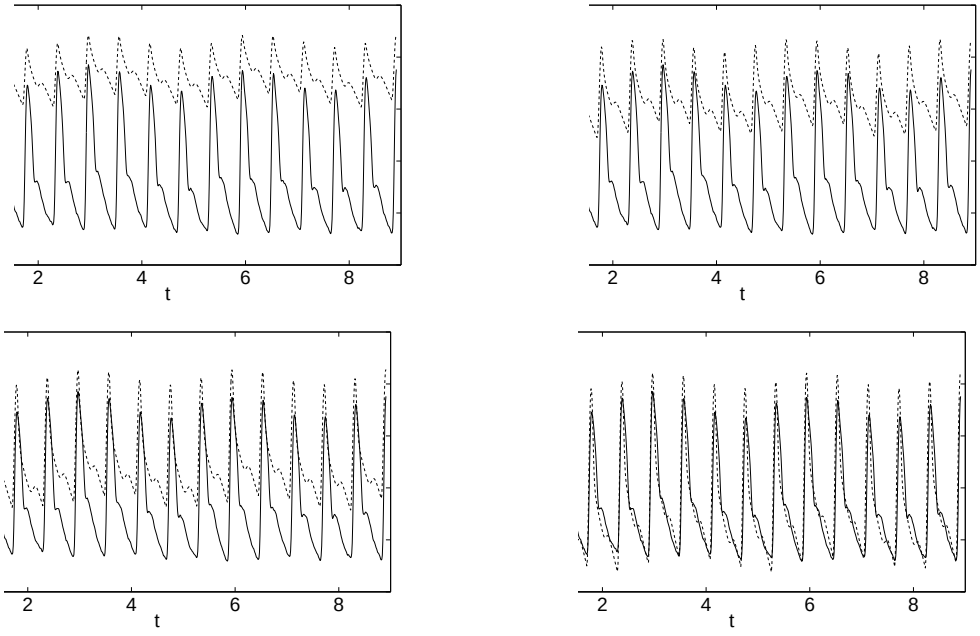

FIGURE 4. Convergence of pressure signals using the Gradient Descent method

This process may be repeated for each parameter and for the corresponding σ expression to obtain two gradient vectors $\nabla\mu, \nabla\sigma$. We choose the vector of parameters $\Theta = (C_v, p_{a0}, C_a, R_c, A)$ with initial value $\Theta_0 = (50, 35, 15, 1.2, 0.5)$ and then iterate as follows:

- Set $\Theta = \Theta_0$ and compute ω_0 and c_2 from the patient's signal.
- Compute δ_μ and δ_σ and then:
  - If $\frac{\delta_\mu}{\mu(\hat{p}_a)} > \frac{\delta_\sigma}{\sigma(\hat{p}_a)}$, $\Theta_{n+1} = \Theta_n - \alpha\nabla\mu$
  - else $\Theta_{n+1} = \Theta_n - \alpha\nabla\sigma$.
- Repeat until the desired tolerance is repeated.

Note, we use a normalised measure, e.g. $\delta(\mu)/\mu$, in the decision process since δ_μ is generally greater than δ_σ. This algorithm is used to improve the estimates for the 5 most important parameters, but it also changes the values of the dependent parameters (so in total 10 are updated). In some cases the calculation did not converge, indicating a poor initial guess however, when convergence was achieved it was typically within 20 iterations. The process is illustrated in Figure 4. The four figures show the 5th, 9th, 13th and 17th iterations. Clearly as the process proceeds the two signals converge, until by the 17th iteration it is clear that the parameter values must be close to the actual values for the patient.

CRM Preprint Series number 1129

4.2.2. *Stage 2: Nelder-Mead method applied to the five significant parameters.* The Gradient Descent method was used to refine the values of the five significant parameters from the values quoted in the literature. We now further refine their values using the Matlab function *fminsearch* which employs the Nelder-Mead method. In this case the objective function was the L_2 distance between the model's output and the recorded arterial pressure,

$$\delta_2 = \left(\int (p_a - \hat{p}_a)^2 \right)^{\frac{1}{2}}. \tag{21}$$

As with the previous two objective functions, this was evaluated over a time period of three respiratory cycles. The initial vector of parameter values were those obtained in the previous stage. The dependent parameters were also re-calculated at each step.

4.2.3. *Stage 3: Nelder-Mead method applied to all parameters.* The method adopted in the previous section was then applied to all parameter values. If stages 1 and 2 are neglected then this approach does not converge. Now that the signals are relatively close convergence is almost always achieved — this will be discussed later. From now on we neglect the interdependence of some parameters. For example, it makes physiological sense to think of E_d as approximately the inverse of C_v, i.e., when the heart is relaxed it is as stiff as a vein, but this may not even be approximately true for certain patients.

At the end of this stage the correspondence between p_a and $\hat{p}_a$ is in general very good with the exception of the dicrotic notch. This is most likely due to minimising the L_2 distance: since the notch takes up only a very small part of the signal the L_2 distance will necessarily be small and so we cannot expect the same level of accuracy to be achieved in modelling the notch as in other parts of the signal.

4.2.4. *Stage 4: Manual refinement.* Given that the model output at this stage is so close to the signal it was decided not to build a new set of objective functions to focus solely on the minor parameters. To be specific the parameters adjusted at this stage were c_4, c_5, c_6 (which describe the notch) and c_1 (which describes the change in elastance height due to respiration). Consequently, for this final refinement we adjusted one parameter at a time up and down by about 1%.

5. Comparison with experimental data

The model results are now compared against three arterial pressure signals taken from the Intensive Care Unit in the Vall D'Hebron hospital, Barcelona. All patients had mechanical ventilation. In the thesis [20] a further six cases are analysed. The patients were categorised as follows:

Patient 1: This patient shows normal values of blood pressure (120/70 mmHg) and heart rate (79 bpm) but a very small dicrotic notch with

CRM Preprint Series number 1129

no real peak. Respiratory variations are small. The patient's pathology was tagged under the category "transplantation".

Patient 2: This patient's pathology was tagged under the category "haemorrhagic". The loss of blood led to low values of blood pressure (85/45 mmHg). Due to this fact they were administered norepinephrine (a vasoconstrictor drug). The heart rate was high (100 bpm), as a natural reaction to the low blood pressure. The dicrotic notch is absent and there is little respiratory variation in systolic pressure.

Patient 3: This patient shows normal values of blood pressure (135/60 mmHg) and normal heart rate (80 bpm) with a large dicrotic notch. Respiratory variations are in the order of 5mmHg in systolic pressure. The patient's pathology was tagged under the category "neurologic". There was also a small dose of vasoconstrictor drugs.

Comparisons of the model output against the arterial pressure for these three patients are displayed in Figures 5–7. The three sets of results show a wide variety of behaviour: high and low pressures, normal and fast heart rates and almost indiscernible to large dicrotic notches. In each case the model replicates the pressure signal very accurately. However, in [20] one case could not be modelled, this was a patient with extremely high blood pressure values (220/85 mmHg) and high heart rate (104 bpm) (labelled Patient 7 in the thesis).

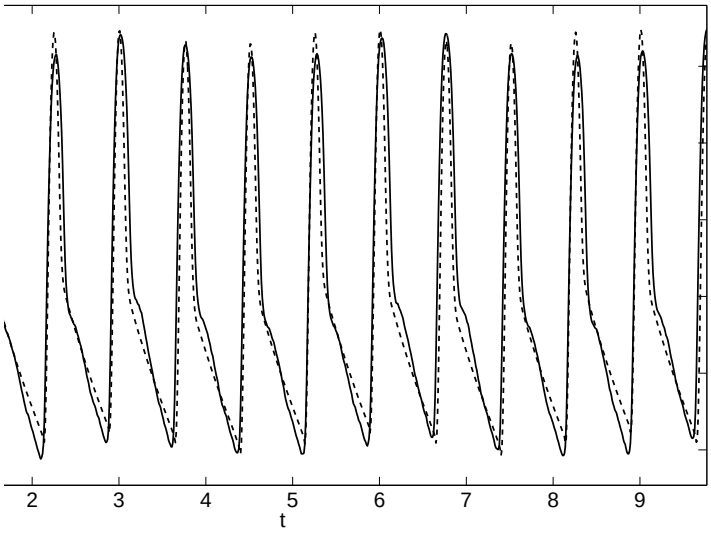

FIGURE 5. Comparison of model (dashed line) and measured (solid line) arterial pressure for Patient 1

CRM Preprint Series number 1129

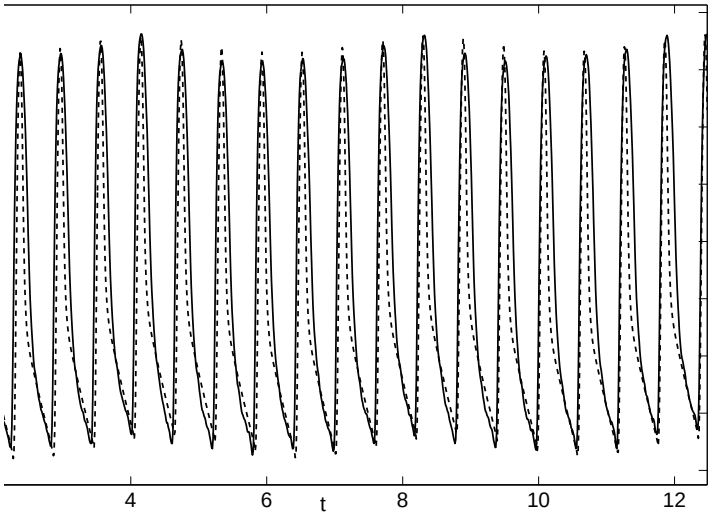

FIGURE 6. Comparison of model (dashed line) and measured (solid line) and measured arterial pressure for Patient 2

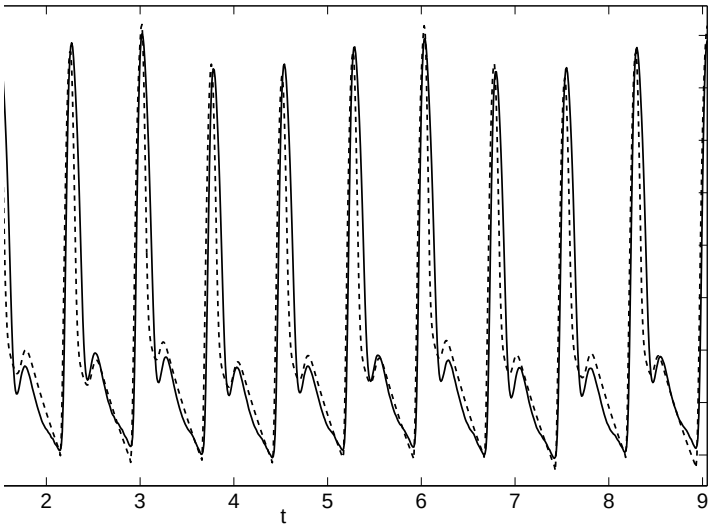

FIGURE 7. Comparison of model (dashed line) and measured (solid line) and measured arterial pressure for Patient 3

CRM Preprint Series number 1129

Parameter	Value	Parameter	Value	Parameter	Value
R_{e0}	0.0055222	p_{a0}	55.0000	E_{s0}	0.57000
R_a	0.020797	p_{v0}	16.628	ϕ	0.33334
R_c	0.41279	p_{LV0}	49.714	R_{eM}	10.009
R_v	0.0055259	ω_0	8.3706	ε	0.00001
C_e	1.6946	c_3	0.00049874	A	0.40341
C_a	2.0000	c_2	4.0153	Δt_0	0.75786
C_v	15.0000	c_1	0.01000	c_4	150.00
p_{e0}	49.896	E_d	0.065511	c_5	18.445
c_6	1.0000				

TABLE 3. Parameter values for Patient 1

Tables 3–5 show the calculated parameter values. It is quite clear that the values in these tables differ significantly from those taken from the literature and provided in Table 1. For example in Table 1 the values $C_v = 59, E_{s0} = 3$ are quoted, the corresponding values from Table 3 are 15 and 0.57. However, this may not be so unusual given that the current data set is taken from patients in the ICU, whereas the data of Table 1 presumably is not. We can also ascertain whether the assumed relations between parameters were justified. The first relation quoted was $C_v = 1/E_d$: from Patient 1 we see $1/E_d = 15.26$, $C_v = 15$. The values of $p_a(0), p_e(0), p_{LV}(0)$ are within 10% etc. Hence, whilst the relationships are not exact they do seem to hold approximately true in general.

6. Conclusion

The results presented in the previous section clearly indicate that our four-compartment model can accurately reproduce a blood pressure signal, with the correct choice of parameter values. The model is capable of accurately reproducing a wide variety of pressure signals. In fact, if the goal is simply a rough characterisation of the blood pressure signal, then the initial stages of the analysis proved sufficient. This showed that the 5 most important parameters in our model are $E_d, E_{s0}, p_a(0), A, R_c$. Provided these are determined accurately, in our case this was achieved through the gradient descent method, then the model will provide a relatively accurate description of the signal.

The four-stage parameter estimation method was vital to the success of the analysis. We have made little effort to optimise this process, since our main goal was to develop and verify the compartment model. However, this provides one direction for future work. For example the final stage involved manual refinement since the L_2 error for the dicrotic notch parameters was small due to the

CRM Preprint Series number 1129

Parameter	Value	Parameter	Value	Parameter	Value
R_{e0}	0.0038808	p_{a0}	17.355	E_{s0}	0.34
R_a	0.0154	p_{v0}	5.7844	ϕ	0.33273
R_c	0.29025	p_{LV0}	17.355	R_{eM}	10.116
R_v	0.0038895	ω_0	10.578	ε	0.000010049
C_e	2.9196	c_3	0.00010007	A	0.4515
C_a	2.9193	c_2	7.003	Δt_0	0.59617
C_v	55.456	c_1	0.006	c_4	0.0000077731
p_{e0}	17.355	E_d	0.0181	c_5	18.436
c_6	4.5053				

TABLE 4. Parameter values for Patient 2

Parameter	Value	Parameter	Value	Parameter	Value
R_{e0}	0.0049252	p_{a0}	21.781	E_{s0}	0.64627
R_a	0.018469	p_{v0}	7.2597	ϕ	0.33338
R_c	0.39929	p_{LV0}	21.761	R_{eM}	10.004
R_v	0.0049253	ω_0	8.3339	ε	0.000010007
C_e	1.54	c_3	0.0001251	A	0.43995
C_a	1.0459	c_2	4.0001	Δt_0	0.75182
C_v	50.000	c_1	0.015	c_4	400
p_{e0}	21.783	E_d	0.029022	c_5	1.000
c_6	3.5000				

TABLE 5. Parameter values for Patient 3

small width of the region. The technique of previous stages could instead be applied to a reduced region around the notch. Employing the Conjugate Gradient method rather than simple Gradient Descent should reduce the number of iterations required.

The motivation for the current work was to use the signal obtained from a pleth (although the source of the signal is irrelevant) and then apply the model to determine a set of parameter values. Based on the output we hope to be able to interpret these parameter values in some way in order to make some recommendation concerning the health of the patient. This will comprise the

CRM Preprint Series number 1129

next stage of this investigation. In order to achieve this we note that the vascular tree can be modelled as a Non-Linear Time-Variant Channel and there are tools that can either linearize this system in order to do the translation from catheter to pleth (Wiener Filters) or just live with these non-linearities and make predictions (Kalman Filters). On the positive side we have a large amount of data both from arterial catheters and the corresponding pleth on which to validate the method.

Acknowledgements

The initial work for this paper was carried out the Centre de Recerca Matemàtica during December 2010 at the Workshop on Mathematical modeling of blood flow and the baroreflex system. We acknowledge the assistance of other participants at that workshop, including Michelle De Decker, Francesc Font, Jonathan Low (all from the CRM) and Dr. Andrew Fowler, Stokes Professor at the University of Limerick, Ireland.

Financial support was provided through a Marie Curie International Reintegration Grant *Industrial applications of moving boundary problems*, grant no. FP7–256417, Ministerio de Ciencia e Innovación grant MTM2011–23789 and the Mathematics Applications Consortium for Science and Industry (`www.macsi.ul.ie`) based at the University of Limerick, funded by the Science Foundation Ireland mathematics initiative grant 06/MI/005.

ASdT would like to thank Dr Ataee of the University of British Columbia for helping sort out the intricacies of the sensitivity analysis.

References

[1] J.F. Augusto, J.L. Teboul, P. Radermacher, P. Asfar, *Interpretation of blood pressure signal: physiological bases, clinical relevance and objectives during shock states*, Intensive Care Medicine **37** (2011), 411–419.

[2] L. Bernardi, F. Keller, M. Sanders, P.S. Reddy, B. Griffith, F. Meno, M.R. Pinsky, *Respiratory sinus arrhythmia in the denervated human heart.* J. Appl. Physiol. **67** (1989), 1447–1455.

[3] G.G. Berntson, J.T. Cacioppo, K.S. Quigley, *Respiratory sinus arrhythmia: Autonomic origins, physiological mechanisms, and psychophysiological implications.* Psychophysiology **30** (1993), 183–196.

[4] Brouse C., Dumont G.A., Boyce W.T., Ataee P., Hahn J.O., *Identification of cardiovascular baroreflex for probing homeostatic stability.* Computing in Cardiology **37** (2010), 141–144.

[5] M. Cannesson et al, *Relation between respiratory variations in pulse oximetry plethysmographic waveform amplitude and arterial pulse pressure in ventilated patients*, Critical Care **9** (2005) R562–R568.

[6] M. Dat, *Modeling cardiovascular autoregulation of the preterm infant.* Thesis Eindhoven University of Technology.

[7] L.M. Ellwein, H.T. Tran, C.Zapata, V. Novak, M.S. Olufsen *Sensitivity Analysis and Model Assessment: Mathematical Models for Arterial Blood Flow and Blood Pressure.* Cardiovasc. Eng. **8** (2008) 94–108. `DOI10.1007/s10558-007-9047-3`

[8] S.J. Chapman, A.C. Fowler, R. Hinch, *An introduction to mathematical physiology.* Mathematical Institute, Oxford University (preprint) 2010. www3.ul.ie/fowlera/courses/bio/physiolbook.pdf

[9] F. Grodins, *Integrative cardiovascular physiology: a mathematical synthesis of cardiac and blood vessel hemodynamics*, Quart. Rev. Biol. **34(2)** (1959), 93–116.

[10] A.C. Guyton, J.E. Hall, *Textbook of medical physiology.* W.B. Saunders Company 2000.

[11] D.R. Hose, A.J. Narracotta, J.M.T. Penrose, D. Baguley, I.P. Jones, P.V. Lawford, *Fundamental mechanics of aortic heart valve closure.* J. Biomechs **39** (2006), 958–967. DOI:10.1016/j.jbiomech.2005.01.029

[12] J. Keener, J. Sneyd, *Mathematical physiology.* Springer 1998.

[13] http://www.cvphysiology.com/BloodPressure/BP004.htm; a website maintained by Richard E. Klabunde, Ph.D., Professor of Physiology, Marian University College of Osteopathic Medicine, Indianapolis, Indiana.

[14] B. Oommen et al, *Modelling time varying elastance: The meaning of load independence.* Cardiovasc. Engng. **3(4)** (2003).

[15] J.T. Ottesen, *Modelling of the baroreflex-feedback mechanism with time-delay*, J. Math. Biol. **36** (1997), 41–63.

[16] J.L. Palladino et al, *Defining ventricular elastance* Proc. 20th IEE conf. in Medicine and Biology.

[17] T.J. Pedley, *Mathematical modelling of arterial fluid dynamics*, J. Engng. Math. **47** (2003), 419444.

[18] M.D. Reisner et al *Utility of the Photoplethysmogram in Circulatory Monitoring* Anesthesiology **108(5)** May 2008.

[19] Patent: System and apparatus for the non-invasive measurement of blood pressure. WO2010043728 (A1) ; ES2336997 (A1). Ribas Ripoll V.J.; Sabirmedical S.L.

[20] A. Saez de Tejada Cuenca. Mathematical modelling of the blood pressure signal. MSC in Mathematics Engng, U. Politecnica Catalunya 2012.

[21] K. Shelley and S. Shelley, *Pulse Oximeter Waveform: Photoelectric Plethysmography,*in Clinical Monitoring, Carol Lake, R. Hines, and C. Blitt, Eds.: W.B. Saunders Company (2001) pp. 420–428.

[22] K.H. Shelley, *Photoplethysmography: Beyond the Calculation of Arterial Oxygen Saturation and Heart Rate*, Anesth. Analg. **105** (2007) S31-S36.

[23] H. Suga, *Cardiac energetics: from emax to pressure-volume area* Clinical and Experimental Pharmacology and Physiology **30** (2003), 580–585.

[24] M. Ursino, *Interaction between carotid baroregulation and the pulsating heart: a mathematical model*, Am. J. Physiol. **275** (Heart Circ. Physiol. 44) (1998), H1733–H1747.

[25] M. Ursino, A. Fiorenzi, E. Belardinelli, *The role of pressure pulsatility in the carotid baroreflex control: a computer simulation study*, Comput. Biol. Med. **26** (1996), 297–314.

Tim Myers, Anna Sáez de Tejada, Vicent Ribas Ripoll
Centre de Recerca Matemàtica
Campus de Bellaterra, Edifici C
08193 Bellaterra, Barcelona
E-mail address: tmyers@crm.cat

Sarah Mitchell
MACSI
Department of Mathematics and Statistics
University of Limerick
Limerick, Ireland

Mark J. McGuinness
School of Mathematics, Statistics and Operations Research
Victoria University of Wellington, New Zealand

CRM Preprint Series number 1129